Adaptive tracking of discriminative frequency components in electroencephalograms for a robust brain–computer interface

Kavitha P Thomas[1]**, Cuntai Guan**[2]**, Chiew Tong Lau**[1]**, A P Vinod**[1] **and Kai Keng Ang**[2]

[1] School of Computer Engineering, Nanyang Technological University, Blk N4, Nanyang Avenue, Singapore 639798
[2] Institute for Infocomm Research, Agency for Science, Technology and Research (A*STAR), 1 Fusionopolis Way, #21-01 Connexis, Singapore 138632

E-mail: kavi0003@e.ntu.edu.sg

Abstract
In an electroencephalogram (EEG)-based brain–computer interface (BCI), motor imagery has been successfully used as a communication strategy. Motor imagery causes detectable amplitude changes in certain frequency bands of EEGs, which are dubbed event-related desynchronization\synchronization. The frequency components that give effective discrimination between different types of motor imagery are subject specific and identification of these subject-specific discriminative frequency components (DFCs) is important for the accurate classification of motor imagery activities. In this paper, we propose a new method to estimate the DFC using the Fisher criterion and investigate the variability of these DFCs over multiple sessions of EEG recording. Observing the variability of DFC over sessions in the analysis, a new BCI approach called the Adaptively Weighted Spectral-Spatial Patterns (AWSSP) algorithm is proposed. AWSSP tracks the variation in DFC over time adaptively based on the deviation of discriminative weight values of frequency components. The classification performance of the proposed AWSSP is compared with a static BCI approach that employs fixed DFCs. In the offline and online experiments, AWSSP offers better classification performance than the static approach, emphasizing the significance of tracking the variability of DFCs in EEGs for developing robust motor imagery-based BCI systems. A study of the effect of feedback on the variation in DFCs is also performed in online experiments and it is found that the presence of visual feedback results in increased variation in DFCs.

(Some figures in this article are in colour only in the electronic version)

1. Introduction

A brain–computer interface (BCI) aims to develop a direct communication and control pathway from the human brain to a computer. This new communication channel does not depend on the brain's normal output pathway of nerves and muscles and it is a promising technology for paralyzed patients to communicate with the external world [1–6].

BCIs based on electroencephalograms (EEGs) use various neurological phenomena, such as visually evoked potentials, slow cortical potentials, P300 potentials and event-related desynchronization (ERD) or event-related synchronization (ERS) during motor imagery in order to translate the user's intent into control signals for external devices. It has been observed that the performance of motor imagery evokes neural activation at the primary motor cortex. Preparation
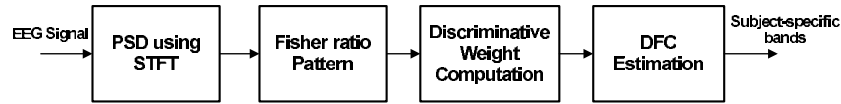
Figure 1. The DFC selection procedure.

for the actual movement or motor imagery is accompanied by a rhythmic power decrease or increase in the primary sensorimotor areas of the brain, which are called ERD\ERS, respectively [7–13]. Based on the antagonistic ERD\ERS patterns, the left- and right-hand motor imagery tasks can be identified.

In order to discriminate motor imagery tasks, common spatial pattern (CSP) [14–20] is an effective feature extraction technique with respect to the topographic patterns of brain rhythm modulations during motor imagery. The most informative frequency bands for discriminating different motor imagery patterns are subject specific. Reports in [12] and [15] state that the selection of these discriminative frequency components (DFCs) is important when extracting features related to motor imagery tasks and for improving the classification accuracy. Therefore, the performance of CSP also heavily depends on its operational frequency bands.

Conventionally, the DFCs of the CSP algorithm were either manually tuned or set to a broad band filter [17]. In order to compute the optimal DFC, the authors in [18] proposed the Common Spatio Spectral Pattern (CSSP) algorithm. CSSP tried to optimize the frequency filters for each channel together with spatial filters. The Common Sparse Spectral Spatial Pattern (CSSSP) algorithm [17] was then proposed to optimize an arbitrary finite impulse response (FIR) filter within the CSP analysis. Sub-band CSP (SBCSP) [19] was later proposed to filter the multi-channel EEG signals using the Chebyshev type 2 infinite impulse response (IIR) filter bank. The algorithm determines the classification capabilities of each frequency band based on the SBCSP features. The Filter Bank Common Spatial Pattern (FBCSP) [20], which employed a fixed filter bank of nine equal bandwidth Chebyshev type 2 IIR filters followed by feature selection and classification algorithms, was then proposed. Subsequently, the Discriminative Filter Bank Common Spatial Pattern (DFBCSP) was proposed in [21] to use subject-specific discriminative filters selected on the basis of Fisher ratio values. The system uses a parent filter bank of 12 FIR filters in the frequency range of 6–40 Hz. The parent filter bank filters the subject's EEG, and the Fisher ratio at each filter output is used to decide the subject-specific filter bank. Then, CSP features are extracted from the filtered EEG for classification.

All of the above-mentioned works in [14–21] focus on the selection of subject-specific DFCs related to motor imagery. But the stability of these subject-specific DFCs over time and its effect on the classification performance of different classes of motor imagery are hardly discussed in the literature.

Therefore, in this paper, we present the following:

(i) A study of the variation in DFCs over various sessions. In order to estimate the DFCs, a new algorithm based on discriminative weight (DW) values of frequency components has been employed.

(ii) The BCI approach named Adaptively Weighted Spectral-Spatial Patterns (AWSSP) tracks the variation in DFCs over time. The DW of each frequency component is computed from the Fisher ratio pattern of EEG signals. In order to demonstrate the impact of tracking the variability in DFCs on the performance of the BCI, a static classification approach that employs fixed bands is also presented for comparison.

(iii) Online and offline experiments to evaluate the proposed BCI approaches.

(iv) Online experiments to study the effect of feedback on the DW values of DFCs.

The paper is organized as follows. Section 2 presents the methodology, including the DFC selection and BCI approaches. The experimental data are discussed in section 3. Section 4 presents an analysis of the offline EEG dataset and discusses the variation in DFCs over the sessions. Section 5 discusses the classification results of offline and online experiments and section 6 offers our conclusions.

2. Methodology

2.1. DFC selection technique

Proper identification of DFCs during various motor imagery tasks (such as left hand and right hand imagery) is important for achieving good classification performance in BCIs [5, 12, 22]. Figure 1 shows the various steps in the proposed DFC selection procedure using DW values. The technique uses the DW values of the EEG signal computed from the time–frequency Fisher ratio pattern for finding out the DFCs. The Fisher ratio is an effective measure of discrimination between two classes of data. In our context, two types of motor imagery are analyzed: the imagination of right hand and left hand movement.

In order to obtain the Fisher ratio values, it is necessary to compute the power spectral density of EEG signals. For every single trial EEG, the power spectral density is computed using the short-time Fourier transform (STFT). A single trial EEG is the multi-channel EEG signal recorded for a certain length of time when the subject is performing motor imagery tasks in response to a visual cue. In the STFT estimation for each single trial EEG, a 256-point FFT is used with a window of length 800 ms and an overlap of 500 ms. Thus, each trial is associated with a discrete time–frequency density pattern $I_n(f, t)$. Then, the Fisher ratio $F_R(f, t)$ is calculated to measure the discriminative power of each time–frequency point across trials and classes,

$$S_W(f, t) = \sum_{k=1}^{C} \sum_{n=1}^{n_k} (I_n(f, t) - m_k(f, t))(I_n(f, t) - m_k(f, t))^T$$

(1)

$$S_B(f, t) = \sum_{k=1}^{C} n_k (m(f, t) - m_k(f, t))(m(f, t) - m_k(f, t))^T \tag{2}$$

$$F_R(f, t) = \frac{S_B(f, t)}{S_W(f, t)}. \tag{3}$$

In equations (1) to (3), S_W, S_B, m_k, m and F_R are two-dimensional matrices where $S_W(f, t)$ and $S_B(f, t)$ represent the within-class and between-class variances, respectively, $m_k(f, t)$ is the average time–frequency density pattern for class k, $m(f, t)$ is the average time–frequency density pattern over k classes where $k = \{1, 2, \ldots, C\}$, and n_k denotes the number of trials for class k. The $DW(f)$ is computed from the time–frequency Fisher ratio pattern F_R as

$$DW(f) = \sum_{t=1}^{T} F_R(f, t), \tag{4}$$

where T represents the number of time segments obtained by the STFT transformation.

After obtaining the $DW(f)$, the band selection algorithm identifies the DFC iteratively. The number of iterations equals the number of bands to be estimated from the $DW(f)$. Initially, the most discriminative band is estimated from the $DW(f)$ using steps 1 to 5 explained here. Then, the second discriminative band is estimated by searching the $DW(f)$ (from steps 1 to 5) avoiding the selected band, i.e. by replacing the weight values of frequency components under the selected band by zero. For example, if the first discriminative band is selected as 8–14 Hz, the second band is estimated from the $DW(f)$ after replacing the DW values for the frequency points 9, 10, 11, 12 and 13 Hz as zero. This procedure is repeated until the desired number of bands are determined. The algorithm for selecting the discriminative band in each iteration is shown in figure 2. In this figure, the steps are separated by downward arrows and are explained here.

Step 1. Initially, a rectangular window of width 3 Hz slides from the frequency point at 6 Hz of the $DW(f)$ to the final point at 40 Hz. The width of the rectangular window is varied from 3 to 9 Hz in steps of 1 Hz, as shown in figure 2. In total, we have seven distinct bandwidth specifications denoted as BW_j, where $\{j = 1, 2, \ldots, 7\}$.

Step 2. We determine the energy distribution α according to equation (5) for every location obtained when sliding the rectangular window along the frequency axis of the $DW(f)$,

$$\alpha(F_i, BW_j) = \sum_{f=f_j - \frac{BW_j}{2}}^{f_j + \frac{BW_j}{2}} DW(f), \tag{5}$$

where F_i stands for the center frequency of the ith band location obtained while sliding the rectangular window along the frequency axis. For example, sliding the rectangular window of width 3 Hz results in 32 band locations, such as 6–9, 7–10, 8–11, \ldots, 37–40 Hz.

Step 3. We estimate the location F_j^{opt} among all locations F_i, which provides maximum energy values α according to:

$$F_j^{\text{opt}} = \arg\max_{F_i} \alpha(F_i, BW_j). \tag{6}$$

This computation is repeated for every BW_j. Thus, for each j, optimum energy measures α_j^{opt} related to center frequencies F_j^{opt} are obtained.

Step 4. We compute the relative change in consecutive α^{opt} values in order to compare the discriminative capability of various BW_j. The relative change δ_j is estimated according to equation (7) for $j = \{2, 3, \ldots, 7\}$. For instance, initially the value of δ_2 is computed using values of α_2^{opt} and α_1^{opt}, as shown in figure 2,

$$\delta_j = \frac{\alpha_j^{\text{opt}} - \alpha_{j-1}^{\text{opt}}}{\alpha_j^{\text{opt}}} \times 100. \tag{7}$$

Step 5. After estimating δ_j values, we compare its values to a threshold of $\delta_{\min}$. The threshold $\delta_{\min}$ is selected from the experimental analysis and is fixed for all subjects. For various values of $\delta_{\min}$, such as 10%, 20%, 30%, 40% \ldots, the bands estimated by the algorithm have been noted and it is found that as the threshold increases, the tendency to select only 3 Hz bandwidth is high. Hence, to incorporate all frequency components in a larger bandwidth, even with a slightly higher discriminative power contribution, the threshold is chosen as 10%. In other words, we compare the value of δ_2 with $\delta_{\min}$ to check whether the increase in bandwidth from $BW_1 = 3$ Hz to $BW_2 = 4$ Hz contains frequency components that contribute to the discriminative power. If $\delta_2 > \delta_{\min}$, we look for the contribution from the next higher bandwidth by computing δ_3 and so on.

The details of steps 4 and 5 are shown in figure 3. The search stops when $\delta_j < \delta_{\min}$ and the $(j - 1)$st location is taken as the first discriminative band, or Band 1. In order to demonstrate the effect of selecting proper DFCs on the classification accuracy of motor imagery tasks, we present the calibration and evaluation procedures for developing a BCI. In both the calibration and evaluation systems, the DFCs are determined based on the DW values of frequency components computed from the Fisher ratio pattern.

2.2. Classification of motor imagery patterns in the BCI

The classification process of BCI tasks includes two phases: calibration and evaluation. During the calibration phase, the subject undergoes a training process and the machine learns a set of subject-specific model parameters from the EEG data recorded. During evaluation, the learned subject-specific model is applied to the new EEG trials to predict which type of imagery activity has been performed. In this paper, the calibration procedure is presented initially, and then two evaluation methods named AWSSP and Static Weighted Spectro-Spatial Pattern (SWSSP) are discussed. SWSSP processes the new EEG signals using the DFC learned from the calibration phase, whereas AWSSP uses the variable DFC learned from new motor imagery patterns. The calibration and evaluation phases are given in sections 2.2.1 and 2.2.2, respectively.
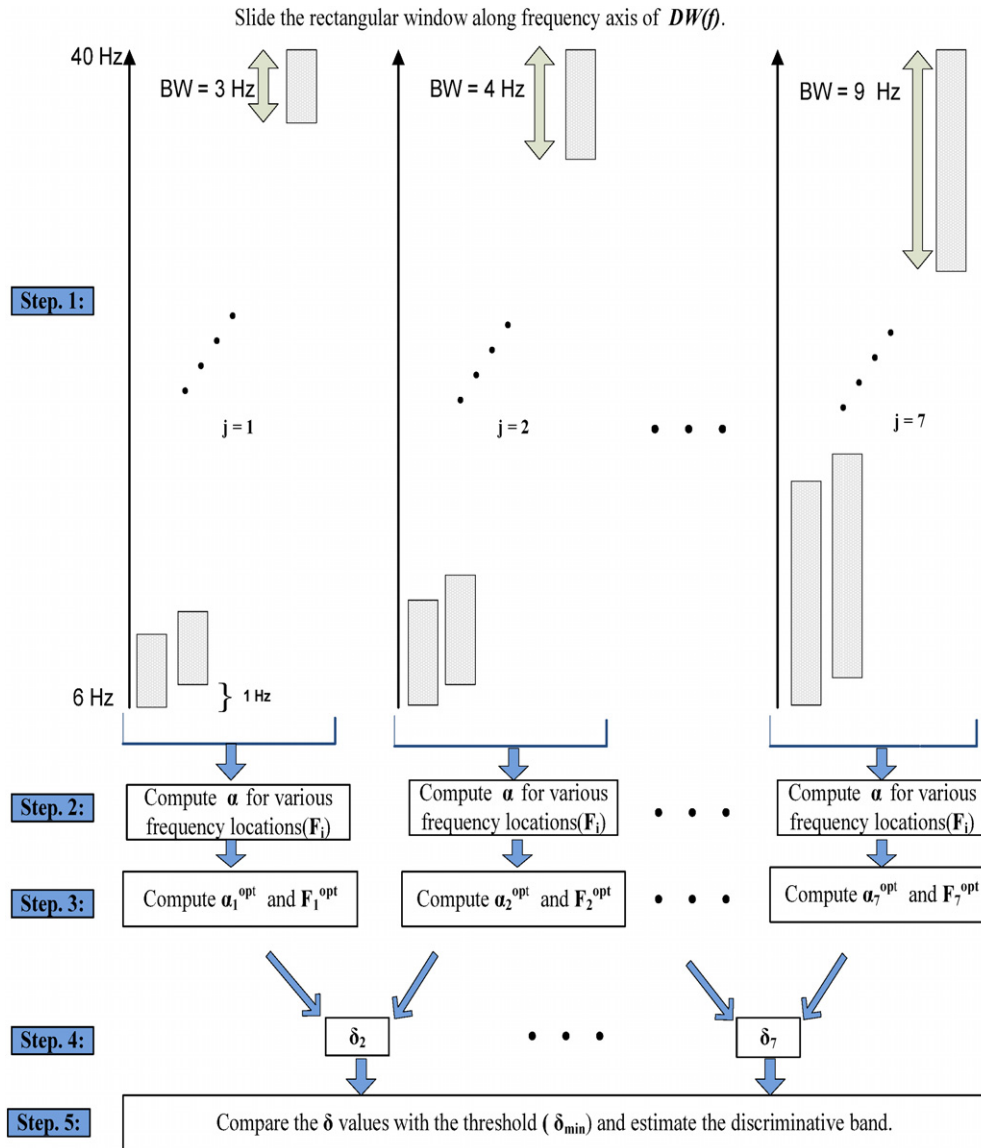
Figure 2. The data flow diagram for the proposed band selection process using DW values. In step 1, rectangular windows of bandwidth varying from 3 to 9 Hz in steps of 1 Hz slide along the frequency axis of DW(f). In step 2, the energy values are estimated according to equation (5). Step 3 selects the optimum frequency location using equation (6) for all bandwidths and step 4 computes δ values according to eqation (7). Step 5 does the comparison of the δ values to estimate the discriminative band.

2.2.1. Calibration phase. The calibration phase has four stages, as illustrated in figure 4. *Stage 1*. Estimate the subject-specific DFC based on the DWs of frequency components.

Stage 2. After getting the frequency bands, design the required bandpass filters using a coefficient decimation technique and filter the EEG.

Stage 3. Apply CSP to the bandpass filtered EEG to extract the features.

Stage 4. Classify the extracted features to predict the task performed. The various steps are presented in the following subsections.

Estimation of DFC. During motor imagery, the EEG signals recorded by electrodes on sensorimotor cortices give the

highest discrimination between various ERD\ERS patterns [13]. Therefore, the proposed method uses the Fisher ratio values of the EEG channel C4 in order to find out the DFC according to the procedure explained in section 2.1. After estimating the DFC, the bandpass filters are designed accordingly.

Bandpass filtering using the coefficient decimation approach. The discriminative bands located by analyzing the DW values are used for the subject-specific filter bank design. For the subject-specific filter design, our work uses a coefficient decimation-based approach proposed in [23] to implement low complexity reconfigurable FIR filters. This technique is a computationally efficient approach to realize FIR filters and has flexible frequency responses. The basic principle of coefficient decimation is as follows. If every Mth coefficient
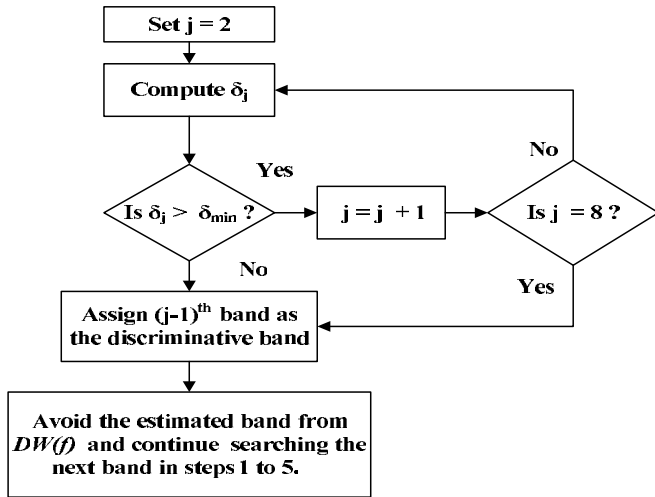
Figure 3. Comparison of δ values in the band selection process. This corresponds to steps 4 and 5 in the DFC selection algorithm.

of an FIR filter $h(n)$ (called the modal filter) is kept unchanged and all other coefficients are replaced by zeros, we get $h'(n)$, which has a multi-band frequency response,

$$h'(n) = h(n)C_M(n), \tag{8}$$

where

$$C_M(n) = \begin{cases} 1, & \text{for } n = kM, \ k = 0, 1, 2, \ldots, M-1 \\ 0, & \text{otherwise.} \end{cases} \tag{9}$$

The frequency response of $h'(n)$ is scaled by M with respect to that of $h(n)$ and the replicas of the frequency spectrum are introduced at integer multiples of $2\pi/M$. By changing the value of M, different numbers of frequency response replicas located at different center frequencies can be obtained. If all of the coefficients of the coefficient decimated filter obtained using equation (8) are grouped together after discarding the in-between zeros, a decimated version of the original frequency response is obtained whose pass-band width is M times that of the original modal filter. If the multi-band frequency responses obtained are selectively masked using inherently low complex wide transition-band frequency response masking filters, different low-pass, high-pass, bandpass and band-stop filters can be obtained. This technique offers good control over the locations of center frequencies and pass-band widths. Depending on the frequency band information from DW values, desired bandpass filters in the BCI system can be obtained by choosing appropriate decimation factors. More details of the coefficient decimation technique can be found

in [23–25]. Thus, the required bandpass filters are designed using the coefficient decimation technique to perform multi-band filtering.

Feature extraction using CSP and classification. The CSP technique allows us to determine spatial filters that maximize the variance of signals of one condition and at the same time minimize the variance of signals of another condition [16]. These spatial filters are obtained by simultaneously diagonalizing the two covariance matrices associated with two populations of EEG signals. The spatially filtered signal Z of a single trial EEG is given by

$$Z = WE, \tag{10}$$

where E is a $C \times S$ matrix representing the raw EEG measurement data of a single trial; C is the number of channels; S is the number of measurement samples per channel; and W is the CSP projection matrix. According to the CSP technique, features from the first and last rows of Z provide maximum discrimination between signals from two classes. Hence, a small number (m) of the first and last rows of Z (Z_p where $p \in 1, \ldots, 2m$) are given as inputs to the classifier. The feature vector F_p is formed according to

$$F_p = \log \left[(\mathrm{var}(Z_p)) \bigg/ \left(\sum_{i=1}^{2m} \mathrm{var}(Z_i) \right) \right]. \tag{11}$$

In this work, the CSP features are extracted from two discriminative filter outputs and therefore each trial is accompanied by four features corresponding to $m = 1$ in the CSP algorithm. Then, features are classified using the naive Bayesian classifier [20].

2.2.2. Evaluation phase. Two evaluation methods are described here for classifying the new motor imagery activities, named AWSSP and SWSSP. The AWSSP and SWSSP algorithms differ in the way they process the new EEG signals. Both schemes adopt the same procedure for learning the subject-specific model.

AWSSP algorithm. Due to the non-stationarity of EEGs and the presence of an oscillating ERD\ERS patterns, the subject-specific DFCs may vary with time during motor imagery [13, 19, 26]. A BCI system is said to be robust if it can keep track of the spectral non-stationarities in the EEG signals. Motivated by this fact, we propose an adaptive method, AWSSP, that tracks the variation in informative bands. The proposed evaluation technique keeps estimating the DW values over time and updates the filtering process adaptively. Figure 5 shows a schematic of the AWSSP algorithm.
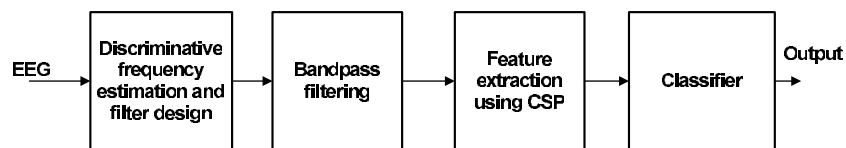

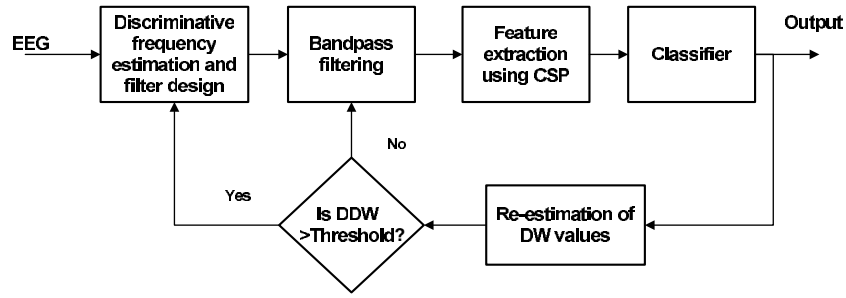**Figure 4.** The framework during calibration.

Figure 5. The framework for the Adaptively Weighted Spectral-Spatial Pattern algorithm (AWSSP) during evaluation.

Before carrying out the evaluation, a subject-specific model is learnt from calibration. The calibration develops the subject-specific bandpass filters, CSP projection matrix for spatial filtering and a classifier model, as explained in section 2.2.1. At the beginning of the proposed evaluation process, a few motor imagery tasks are processed using the same model parameters learnt from the calibration session. We have fixed the number of tasks processed in the calibrated parameters as 40 because it is found that about 30 or 40 tasks are required to give a fair estimate of DW values. Therefore, until the 40th task in evaluation sessions, the classifier model, CSP transformation matrix and bandpass filters are fixed. After the 40th task, the DW values are re-computed from these 40 trials. Then, these updated DW values are deviated from the calibrated DW values. This percentage deviation in DW (DDW) is computed according to

$$\frac{\sum_{n=1}^{N_{\text{bands}}} \sum_{k=-\text{BW}/2}^{\text{BW}/2} [\text{DW}_i(f_n+k) - \text{DW}_{i-1}(f_n+k)]}{\sum_{n=1}^{N_{\text{bands}}} \sum_{k=-\text{BW}/2}^{\text{BW}/2} \text{DW}_{i-1}(f_n+k)} \times 100,$$

(12)

where N_{bands} is the number of bands estimated (here it is 2) and f_n is the center frequency of the nth band. DW_i and DW_{i-1} represent the DW values in the ith and $(i-1)$st trial. At the end of the ith trial, the deviation in the DW of the current bands is estimated using the above equation. When DDW is greater than or equal to the threshold, the frequency bands are estimated from the DW_i values. Consequently, the bandpass filters in the system are reconfigured. The $(i+1)$st trial is processed using the updated bands. If DDW is less than the threshold, current bands are used for the next tasks too, without any updates. The same procedure is repeated for the subsequent EEG signals in every single trial too.

The various steps in the evaluation phase of the AWSSP algorithm upon receiving a new single trial EEG during a motor imagery task are summarized here in steps 1 to 10. This procedure is fixed for both offline and online experiments presented in this paper. Before proceeding to the classification of a new EEG trial (E) in the evaluation, the subject-specific model has to be learnt through calibration. In the explanation given, n represents the index of motor imagery task or the received single trial EEG matrix E of size $C \times S$, where C is the number of channels and S is the number of time samples.

Steps to perform the AWSSP algorithm:

(*1*) *Initialize the index of the new single trial EEG* (E) *as* $n = 1$.

(*2*) *Filter the EEG in the given single trial* (E) *using the selected bandpass filters, extract the CSP features* (*using equations* (*10*) *and* (*11*) *in section Feature extraction using CSP and classification*) *and predict the task performed using the classifier*.

(*3*) *Compute the power spectral density of the data E using STFT and save it in the left/right power spectral density matrix depending on the predicted/true class label*.

(*4*) *If* $n < 40$, *go to step 9. If* $n \geqslant 40$, *go to step 5. This is because the algorithm starts updating its model parameters only after receiving 40 motor imagery trials in the evaluation phase*.

(*5*) *Compute the new* DW (f)*according to equations* (*1*)−(*4*) *from the saved power spectral density matrix of the previous 40 motor imagery tasks*.

(*6*) *Calculate* DDW *as per equation* (*12*) *by comparing the existing and new* DW(f) *values*.

(*7*) *If the* DDW *is greater than the threshold, go to step 8. Otherwise, no updates are done; proceed to step 9*.

(*8*) *Update frequency bands from the new* DW(f) *based on equations* (*5*)−(*7*). *Reconfigure the bandpass filters according to the updated bands and retrain the classifier using the features from the previous tasks*.

(*9*) *Wait for the next trial*.

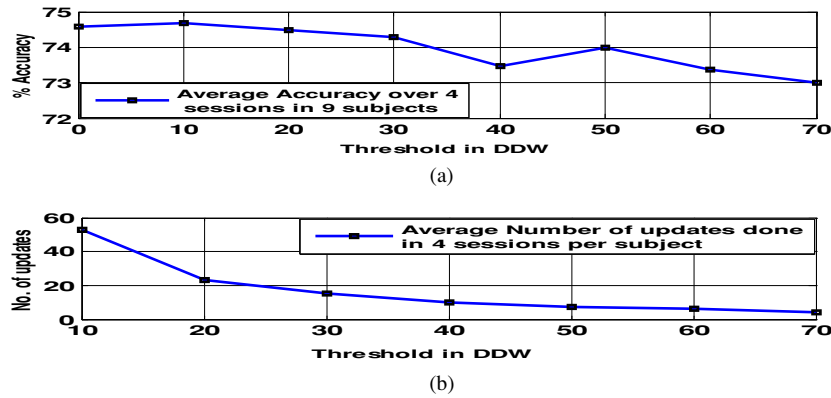(*10*) *When a new EEG is received, $n = n + 1$; proceed to step 2*.

Figure 6. Effect of the threshold chosen on the performance of AWSSP$_{sup}$: (a) variation in classification accuracy versus the threshold in DDW and (b) variation in number of updates done versus the threshold in DDW.

The threshold mentioned in step 7 of the algorithm stands for a minimum value of deviation (DDW) allowed in the DW values of existing frequency components. This is determined from the experimental analysis and is fixed for all subjects. In order to study the effect of the threshold set for DDW on the classification performance of motor imagery tasks by AWSSP$_{sup}$, the classification accuracies of the algorithm are noted for various values of the threshold. Figure 6(a) shows the average percentage accuracy of classification for nine subjects in the four evaluation sessions of BCI competition IV dataset IIb [27] for different threshold values. The details of the data are presented in section 3.1. In order to find the threshold setting that gives good performance with fewer updates, its value is varied from 0% to 70%. If DDW > threshold, the bandpass filters and classifer are updated. Obviously, as the threshold value decreases, the number of updates done will increase. Figure 6(b) shows the number of updates done over four evaluation sessions per subject for various threshold values. From the analysis, we fixed the value of the threshold as 30% for all subjects in our analysis as it gives a comparable performance with fewer updates compared to threshold values of 10% and 20%.

In AWSSP, the DFC and classifier are updated using either the true labels or the predicted labels. These two evaluation methods are termed as supervised AWSSP (AWSSP$_{sup}$) and unsupervised AWSSP (AWSSP$_{unsup}$), respectively, in the sequel. These algorithms update the DWs of frequency components when new EEG tasks are received. Based on the DDW values, the bands from updated weight information are used for processing the new task. In both AWSSP$_{unsup}$ and AWSSP$_{sup}$, the classifier is retrained using previous features whenever the bands are updated.

SWSSP algorithm. In SWSSP, the model parameters developed during calibration are fixed during evaluation also, without any updates. The subject-specific bandpass filters, CSP transformation matrix for spatial filtering and classifier model used for new EEG samples are the same as those developed during calibration. Classification accuracies of this static algorithm can be compared to AWSSP in order to demonstrate the impact of tracking the DFC on the classification performance of a BCI system.

3. Experimental data

The proposed methods are analyzed using offline and online experiments. The offline analysis is done using the publicly available BCI competition IV dataset IIb [27]. In the online experiments, the performance of three subjects are analyzed.

3.1. Offline data

The offline data, the BCI competition IV dataset IIb, were collected from nine normal right-handed subjects performing left and right motor imagery tasks. Three bipolar EEG measurements were recorded from electrodes C3, Cz and C4, and sampled at 250 Hz. They were bandpass filtered between 0.5 and 100 Hz, and a notch filter at 50 Hz was enabled. During motor imagery, subjects were sitting in an armchair, watching a screen monitor placed approximately 1 m away at eye level. The cue-based data-recording paradigm consisted of two classes, which were motor imagery of the left hand and the right hand. Each trial started with a fixation cross on the screen with an additional short acoustic warning tone (1 kHz, 70 ms). A few seconds later a visual cue (an arrow pointing to the left or right, according to the required class) was presented for 1.25 s. Afterwards, the subjects had to imagine the corresponding hand movement over a period of 4 s.

The data for each subject comprise five sessions of EEGs recorded over different days. Each of sessions 1 and 2 has a total of 120 motor imagery trials, with 60 left and 60 right hand motor imagery trials per session. There are 160 trials in each of sessions 3, 4 and 5, having 80 repetitions of both left and right hand motor imagery tasks per session. The exceptions are session 4 of subject 2 with 120 trials, session 2 of subject 4 with 140 trials, and session 2 of subject 4 with 140 trials.

3.2. Online experiments

The online experiments were conducted at the Institute for Infocomm Research, Agency for Science, Technology and Research, Singapore, using the Neuroscan NuAmps 32 channel EEG amplifier. Recorded EEGs were bandpass filtered between 0.5 and 100 Hz and a notch filter of 50 Hz was enabled. The sampling rate was set to 250 Hz. EEG
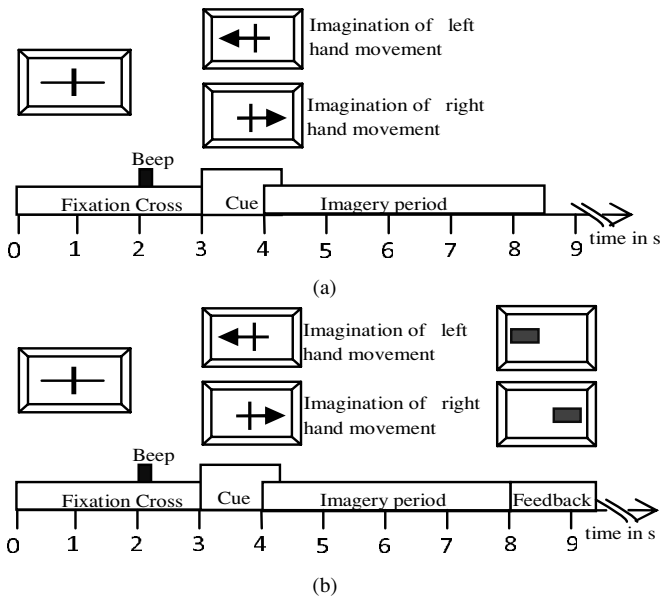
Figure 7. The timing protocol for online experiments: (a) during calibration and (b) during evaluation with feedback.

signals were recorded using 25 electrodes around the motor cortex, which were F7, F3, Fz, F4, F8, FT7, FC3, FCz, FC4, FT8, T7, C3, CZ, C4, T8, TP7, CP3, CPz, CP4, TP8, P7, P3, Pz, P4 and P8. EEG data were taken from three subjects, and for each subject data collection was performed on three different days with an interval of a few weeks. After learning the calibration model, three sessions of EEGs were recorded each of 120 trials, consisting of 60 left and 60 right hand movement imaginations for each subject.

During data collection, the subject was sitting in a comfortable armchair 150 cm in front of a computer monitor and was instructed not to move, and to keep both arms and hands relaxed. The timing protocol for calibration and evaluation is shown in figures 7(a) and (b), respectively. As shown in figure 7(a), the experiment started with a display of a fixation cross that was shown in the center of the monitor. After 2 s, a warning stimulus was given in the form of a beep. From 3 to 4.5 s, an arrow pointing toward the left or right was shown on the monitor. The subject was instructed to imagine a left or right hand movement for 5 s, depending on the direction of the arrow. Each trial was followed by a short break of at least 1.5 s. Using the calibration session, a subject-specific model was learnt for each subject as explained in section 2.2.1. This model was used to evaluate new EEG signals recorded in the online sessions.

For the evaluation session, the subject was instructed to imagine left or right hand movement according to the cue displayed. As given in figure 7(b), the subject performed motor imagery between 3 and 8 s, depending on the cue. Between 8 and 9 s, the EEG was classified online and the classification result was translated into a feedback stimulus in the form of a horizontal bar that appeared in the center of the monitor. If the person imagined a left hand movement, then the bar varying in length extended to the left, as shown in figure 7(b). Assuming correct classifications in figure 7(b), horizontal feedback bars have been shown toward left and right for left and right hand motor imagery tasks, respectively. The length of this feedback bar depends on the confidence score of classification of the corresponding task. The time interval between two trials was 1.5 s. The online experiments with feedback were conducted on three different days for all subjects. Accordingly, the experiments were divided into three sessions. The part of the whole online experiments conducted in one single day is referred to as a 'session'. In each session, adaptive and static evaluations of EEG signals were performed separately. The details are as follows.

3.2.1. Session 1.　The first online evaluation session was conducted on the same day as the calibration for each subject. After developing a subject-specific model according to the procedure explained in section 2.2.1, the new trials were processed with and without incorporating spectral updates over time. In session 1, the first set of 120 motor imagery trials (including 60 left and right hand trials) was processed and classified online using the calibration model parameters (using SWSSP). The next set of 120 motor imagery trials was evaluated by the adaptive algorithm, addressing the spectral non-stationarity over time (using AWSSP$_{sup}$). In AWSSP$_{sup}$, the first 40 motor imagery tasks were processed using the calibrated model parameters. The following EEG samples were evaluated by employing the filtering and classifier updates based on the procedures explained in section 2.2.2.

3.2.2. Session 2.　The second stage of experiments, or session 2, was conducted around 5 weeks after the session 1 experiments. In session 2, we did the adaptive and non-adaptive evaluations of motor imagery trials using the AWSSP$_{sup}$ and SWSSP algorithms, respectively. By performing repetitive left or right hand motor imagery tasks, the subject may adaptively learn his or her own optimum strategy to improve the classification performance. In order to minimize the effect of bias that may creep in due to this subject adaptation along with machine adaptation, we performed the adaptive evaluation first and the static evaluation later, in session 2. The experiments in session 2 were conducted under the same experimental setup as that of session 1 for each subject. The results of the experiments are discussed in section 5.2.

3.2.3. Session 3.　Both the static and adaptive evaluations in sessions 1 and 2 were performed with feedback only. The study in [12] reports that the relevant frequency bands can change due to the visual feedback as the subject may try to optimize his or her strategy with feedback, leading to changes in EEG patterns. Therefore, one more online experimental session (session 3) was also performed in order to investigate the effect of feedback on the variation in the DFC. In this session, experiments were conducted with and without feedback using static and adaptive evaluation techniques. The specific aim of this session was to study the effect of feedback on the variation of DDW values of frequency components. At first, the subject was presented with a set of 120 motor imagery trials (60 left and 60 right) without providing feedback and then another set
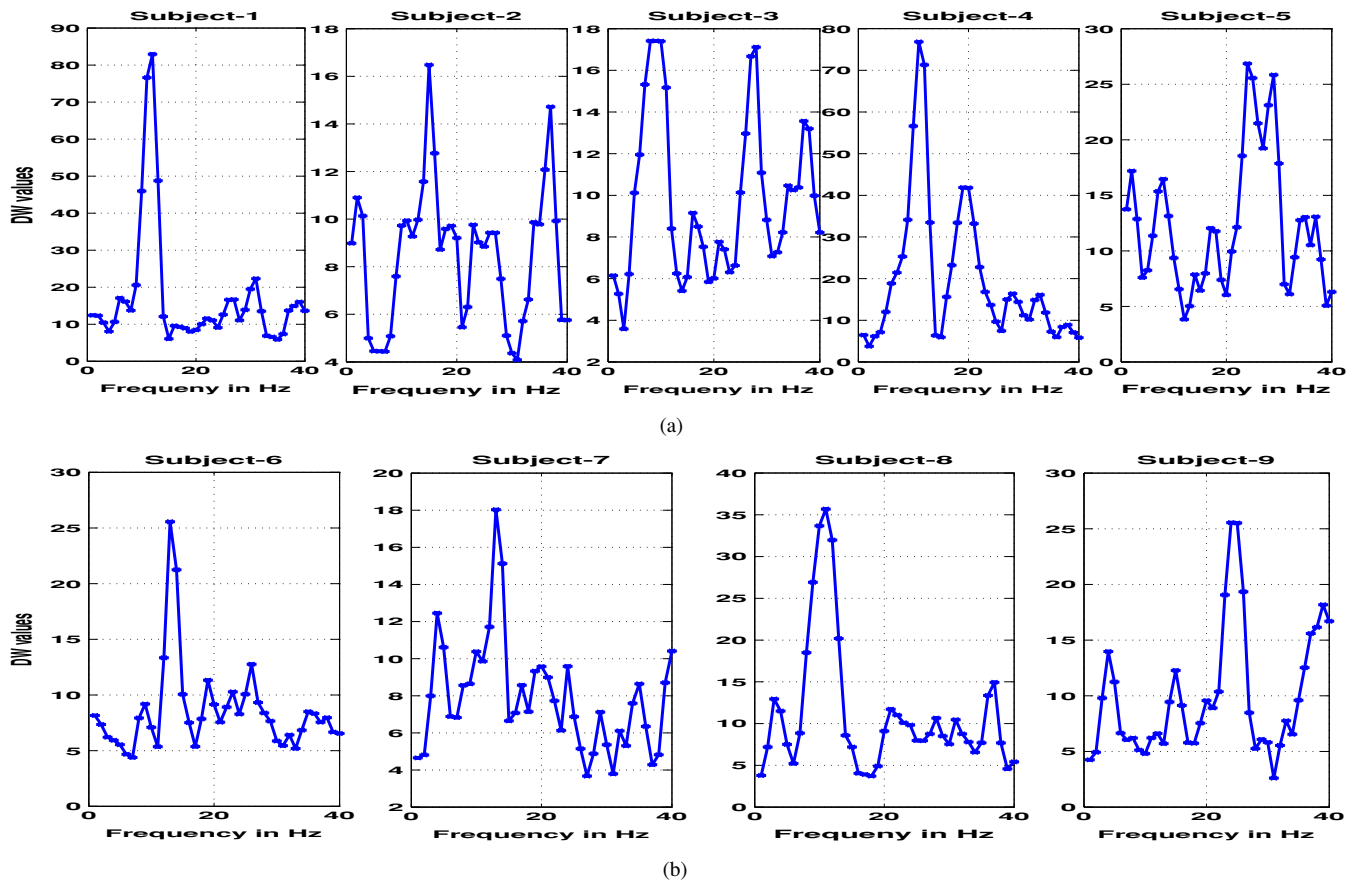
Figure 8. DW values for session 1 in subjects 1–9 of BCI competition IV dataset IIb: (a) for subjects 1, 2, 3, 4 and 5 and (b) for subjects 6, 7, 8 and 9.

Table 1. The selected frequency bands for the nine subjects.

Subject	S1	S2	S3	S4	S5	S6	S7	S8	S9
Band 1 (Hz)	10–14	11–17	7–12	10–13	24–30	12–15	10–15	9–13	23–27
Band 2 (Hz)	8–11	34–39	25–30	18–22	22–25	19–27	17–25	7–10	36–40

of 120 trials along with feedback. The signals were processed and classified using the adaptive scheme. Finally, one more set of 120 trials was recorded with feedback, and classified using the static scheme. During the experiment, the deviation in DW values was computed for every new bunch of 30 single trial motor imagery EEGs according to equation (12), compared to the DW values obtained during the calibration phase. This has been done for all EEGs recorded in session 3 and the experimental results are provided in section 5.2.

4. Offline data analysis

In order to investigate the discriminative spectral variability during the performance of motor imagery, the DFC in various sessions of BCI competition IV dataset IIb [27] are analyzed here. The dataset consists of five sessions of EEG recorded from nine subjects and each session is analyzed separately using the respective DW function.

4.1. Selection of DFC from DW values

The DFCs have been effectively located by the proposed band selection algorithm explained in section 2.1 and can be used in the automatic estimation of frequency bands in BCI applications. The plots in figures 8(a–c) show the variation in the DW values with frequency components for nine subjects in the BCI competition IV dataset IIb in session 1. The band selection algorithm effectively locates frequency components with higher DW values and the estimated bands from the DW values are given in table 1.

Based on the experimental analysis, the number of bands is fixed as 2 in the study and increasing the number of bands did not provide a noticeable improvement in the classification performance. Also, the criterion level δ_{min} is chosen as 10 for all subjects from the analysis. The bands of relative change less than δ_{min} are eliminated as the corresponding frequency components do not contribute much to the discriminative energy distribution of the Fisher ratio pattern.
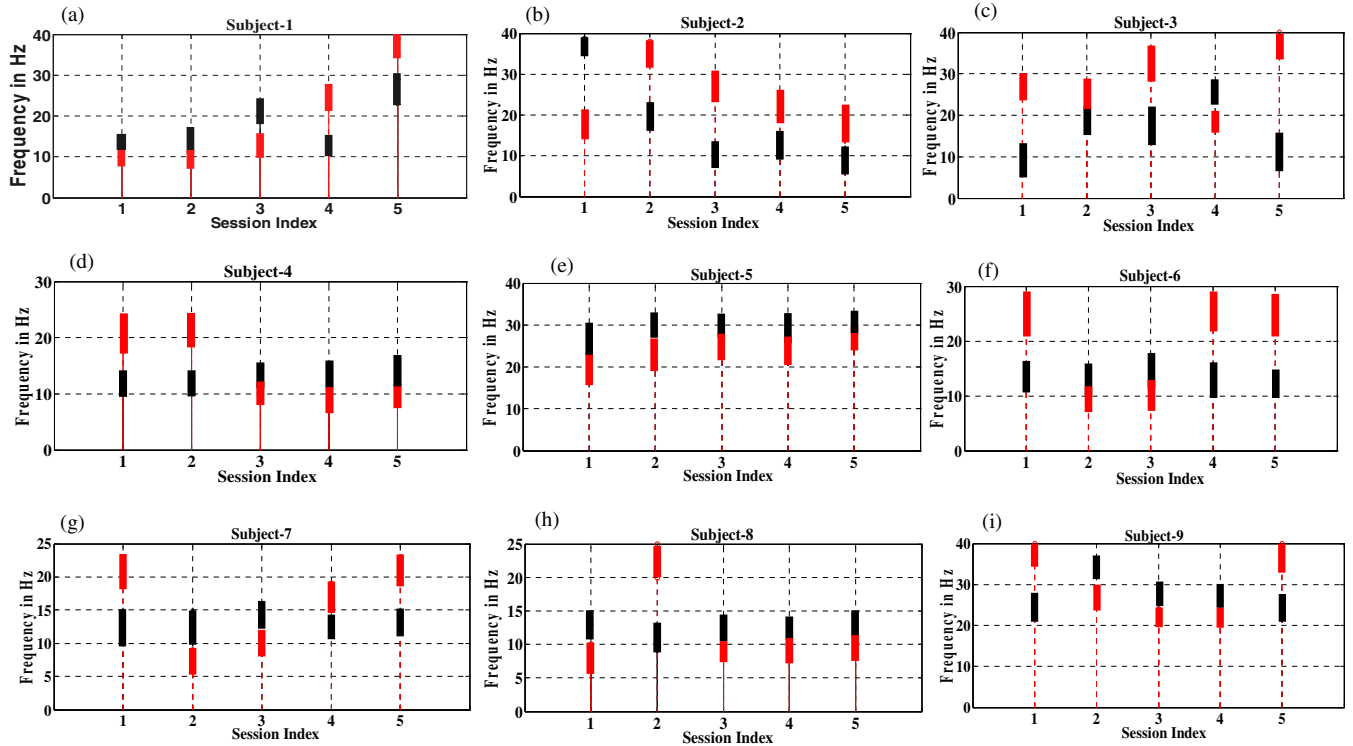
Figure 9. Variation in DFCs in five sessions for nine subjects. The black and red plots represent the first and second most discriminative bands respectively for the corresponding session. The *x*-axis represents sessions 1, 2, 3, 4 and 5 and the *y*-axis is the frequency in Hz.

4.1.1. Inter-session variability in DFCs. In order to analyze the discriminative spectral variability over various sessions, the 10-fold cross-validation procedure is performed in each of the five sessions independently in a trial-based manner. Each 10-fold cross-validation divides the single trials of each session into ten equal partitions. Each part comprises 12 complete single trials of data. The data samples in each single trial are always kept together and data samples among trials are never mixed. In the cross-validation of each session, the single trials of one partition are used for testing while the remaining nine partitions are used for training. Therefore, the samples present in test data never appear in the training data. From each training set, we develop two discriminative frequency bands that are used for bandpass filtering the EEG signals in the test set. From each of the training sets in the 10-folds, 10 sets of frequency bands (total 20 bands) are estimated. Then, the fold-specific bands are noted and the number of times each band appears is computed. The first and second discriminative bands are selected based on the number of times they are selected in all folds, i.e. the most frequent band is selected as the first discriminative band.

The 10-fold cross-validation is done on all sessions individually and the two discriminative bands are noted. Figures 9(a–i) show the selected discriminative bands in five sessions for subjects 1 to 9, respectively. The black and red plots in figure 9 represent the first and second most discriminative bands, respectively. After choosing the session-specific discriminative bands (based on the procedure explained in section 2), the 10-fold cross-validation procedure is repeated by processing all of the folds in these two selected

frequency bands in the respective sessions for all subjects. Features from these two selected discriminative bands gave similar or higher classification accuracies in most of the sessions in all of the subjects compared to fold-specific bands. Hence, the selected bands plotted in figure 9 represent the discriminative spectral information in all sessions.

Figure 9 reveals significant inter-session variation in DFCs in all subjects. But the degree of discriminative band variation is found to be subject specific. For example, in subject 1, the selected bands for sessions 1, 2, 3, 4 and 5 are {11–14 and 9–12 Hz}, {10–14 and 8–11 Hz}, {19–23 and 11–14 Hz}, {11–14 and 22–26 Hz} and {23–29 and 35–39 Hz}, respectively. Similarly, in all nine subjects, the discriminative bands vary from session to session. Hence, the variability in frequency bands over time should be addressed in a BCI to improve the performance. The following section provides classification results of online and offline datasets using the AWSSP and SWSSP algorithms.

5. Classification results and discussion

5.1. Results of offline data

Among the five sessions available in the competition dataset, the first session is used for calibration and the other four sessions are taken for evaluation. After performing the calibration, sessions 2, 3, 4 and 5 are evaluated using the SWSSP and AWSSP methods.

In order to find the optimal channel for the band selection process, the classification accuracies for various channel selection possibilities have also been investigated. The average
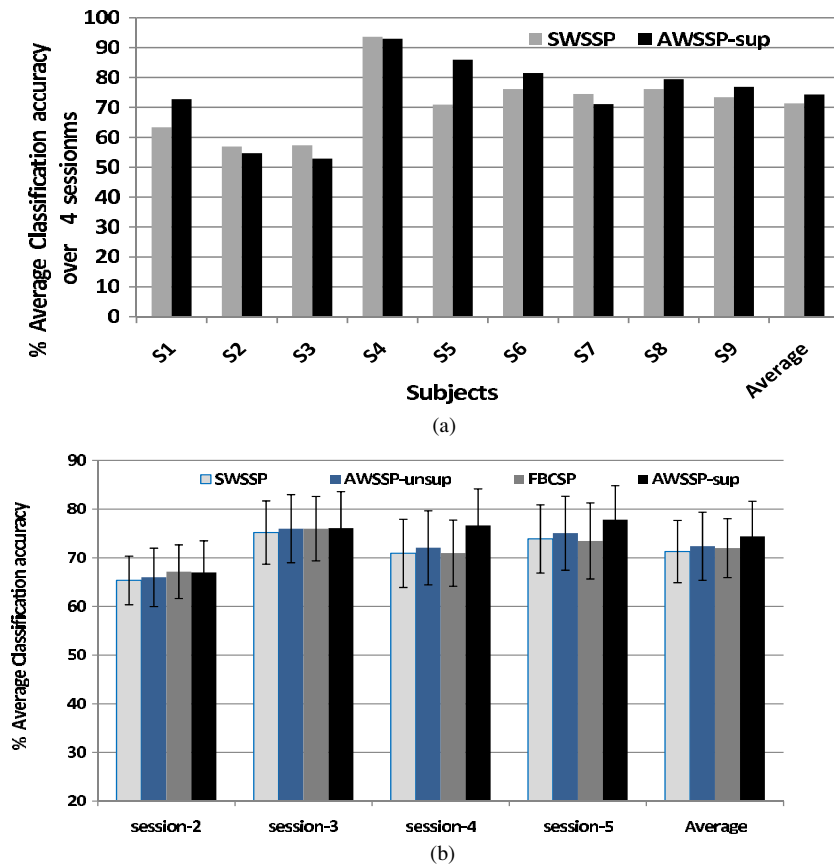
(a)

(b)

Figure 10. Comparison of classification accuracies using SWSSP, AWSSP and FBCSP: (a) in nine subjects and (b) in five sessions.

Table 2. Average classification accuracy in nine subjects over four sessions with channels used for band selection.

Channel	C3	Cz	C4	C3, Cz and C4
Average accuracy	71.29%	69.25%	74.30%	68%

classification accuracies in the dataset using $AWSSP_{sup}$ are presented in table 2. As the classification accuracy obtained for C4 is better than that of other channels, we fixed C4 as the band selection channel for our experiments.

Figure 10(a) shows the average accuracies over four sessions for all nine subjects. The results show that the proposed $AWSSP_{sup}$ method performs better than SWSSP in most of the subjects. $AWSSP_{sup}$ outperforms SWSSP because it tracks the variation in informative frequency components over time. Making use of the true labels, $AWSSP_{sup}$ performs better than $AWSSP_{unsup}$, which depends on the predicted class labels only. The classification performances using our proposed algorithms SWSSP, $AWSSP_{sup}$ and $AWSSP_{unsup}$ and FBCSP [20] are presented in figure 10(b). FBCSP is the winning algorithm of the BCI competition IV held in 2008 for the discussed dataset IIb. Figure 10(b) shows the average classification accuracies and standard deviation over nine subjects in four evaluation sessions. It is found that, on average, the proposed $AWSSP_{sup}$ method outperforms all of the other methods listed here. The statistical analysis of the classification accuracies obtained in the four evaluation sessions by $AWSSP_{sup}$ gives a two-tailed *p* value of 0.002 in

a paired *t*-test compared to the results obtained by SWSSP. Even though the classification performance of $AWSSP_{sup}$ is better than $AWSSP_{unsup}$ and FBCSP, more effective techniques have to be developed in future to obtain statistically significant performance enhancement.

5.2. Results of online data

In the online study, the thresholds in the DDW and EEG channel selected for band selection are consistent with those used in the offline evaluation also. The threshold in DDW is kept as 30% and the bands are estimated from the EEG channel C4.

5.2.1. Results of sessions 1 and 2. Three subjects named SG, SM and SS participated in the online experiments. The subject-specific model learnt from the calibration session evaluates the EEG signals recorded in the new online sessions with and without adaptation. The results of the online experiments are tabulated in table 3. Sessions 1 and 2 in table 3 represent the experiments conducted on two different days, separated by almost 5 weeks. In both sessions, 120 motor imagery trials were evaluated adaptively as well as 120 trials non-adaptively, using $AWSSP_{sup}$ and SWSSP, respectively. In sessions 1 and 2, the adaptive evaluation of all three subjects provide higher classification accuracies than when using the static method. In session 2, the adaptive evaluation offers an average accuracy of 86.11% whereas it is 80.11% without adaptation, even though

Table 3. Classification results of online data for three subjects in sessions 1 and 2.

Session	Session 1		Session 2	
Subject	Static	Adaptive	Static	Adaptive
SG	86.25%	91.25%	87.50%	90%
SM	87.50%	92.50%	85%	93.75%
SS	81.25%	85%	78.75%	81.25%
Average	85%	89.58%	83.75%	88.33%

Table 4. Details of the online updates in subject SM in session 1.

Index of trial	DDW	Updated bands	Processing time
40	38.50%	15–19 and 10–14 Hz	250 ms
55	31.86%	10–17 and 28–34 Hz	271 ms
74	32.00%	7–14 and 16–20 Hz	248 ms
114	32%	9–13 and 15–20 Hz	237 ms

Table 5. Details of the online updates in subject SG in session 1.

Index of trial	DDW	Updated bands	Processing time
40	59.35%	13–17 and 19–25 Hz	280 ms
60	31.45%	10–17 and 22–29 Hz	271 ms
84	31.03%	20–27 and 9–15 Hz	242 ms
112	31.15%	8–12 and 16–21 Hz	236 ms

Table 6. Details of the online updates in subject SS in session 1.

Index of trial	DDW	Updated bands	Processing time
40	37.10%	9–12 and 31–37 Hz	278 ms
85	63.03%	10–13 and 15–18 Hz	264 ms
100	30.83%	9–13 and 17–23 Hz	270 ms

Table 7. Details of the online updates in subject SM in session 2.

Index of trial	DDW	Updated bands	Processing time
40	46.18%	15–20 and 7–13 Hz	260 ms
61	31.86%	8–14 and 16–23 Hz	256 ms
98	32.21%	9–14 and 18–24 Hz	236 ms
113	30.80%	9–13 and 14–21 Hz	253 ms

Table 8. Details of the online updates in subject SG in session 2.

Index of trial	DDW	Updated bands	Processing time
40	55.38%	15–21 and 9–16 Hz	265 ms
62	33.97%	9–13 and 18–24 Hz	250 ms
78	32.10%	20–27 and 7–12 Hz	236 ms
99	34.70%	9–14 and 19–25 Hz	236 ms

Table 9. Details of the online updates in subject SS in session 2.

Index of trial	DDW	Updated bands	Processing time
40	51.17%	9–13 and 14–18 Hz	265 ms
59	31.40%	10–13 and 37–40 Hz	240 ms
68	35.43%	10–13 and 28–33 Hz	245 ms
98	33.17%	10–13 and 6–10 Hz	254 ms

session 2 was done 5 weeks after the subject-specific model development.

It is observed that the adaptive method consistently shows improvement in all of the subjects. This shows the effectiveness of adaptive tracking of the spectrum variations over time, by the proposed method. For the adaptive method AWSSP$_{sup}$, as mentioned in section AWSSP algorithm, until the 40th trial, the signals are processed using the calibrated model and DW values are re-computed after the 40th trial. Then, the filtering and classifier updates are done based on the DDW values computed according to equation (12). Whenever DDW is greater than 30%, the bandpass filters and the classifier model are updated. Therefore the values given in table 3 are the classification accuracies out of 80 trials in static and adaptive methods. The first 40 trials have not been considered in computing accuracy as they are classified before adaptation in the adaptive method.

During calibration for subject SM, 9–15 and 20–24 Hz were selected as the two discriminative frequency bands. When new samples were received, four updates were done in the adaptive evaluation of session 1 to track the variations in the signal and the details are shown in table 4. The time taken for displaying the feedback by the algorithm after receiving the input EEG is also provided to show the feasibility of the proposed method in real time applications. The processing time mentioned here is using an Intel(r)Xeon(R) 2.00 GHz processor of 3.25 GB RAM. In session 2 of subject SM, the adaptation of frequency bands offers an accuracy of 93.75% whereas it is 85% using the static method. The online updates of DFC and DDW values for all three subjects SM, SG and SS in the two sessions have been provided in tables 4 to 9.

Considering the performance of all three subjects, the average times for processing a single trial with and without

updates are 250 and 110 ms, respectively. However, the online updates are found to be effective in improving the classification accuracies. Also, comparing the online adaptive and non-adaptive evaluation results of the subjects SG, SM and SS in two sessions, the paired *t*-test provides a two-tailed *p* value of 0.005. The online and offline results reflect the significant performance improvement by the adaptive method over the static, and emphasize the importance of tracking the non-stationary EEG spectral components in real time BCI applications based on motor imagery.

5.2.2. Results of session 3: effect of feedback on DDW. The study of the effect of feedback on the variation in DFCs is performed by computing the DDW values for every new bunch of 30 motor imagery trials received in each EEG recording. After estimating DW values for every bunch, the DDW of these DW values compared to the subject-specific DW values obtained during calibration are estimated. Hence % DDW values are estimated at trials 30, 60, 90 and 120. This computation is repeated for all three subjects in the EEG recordings with and without feedback. Figure 11 shows the % DDW values for subjects SG, SM and SS with and without feedback for EEG signals evaluated by the adaptive method. It is observed from the figure that the deviation in DW values in EEGs is higher in all subjects with feedback compared to the signals without feedback.
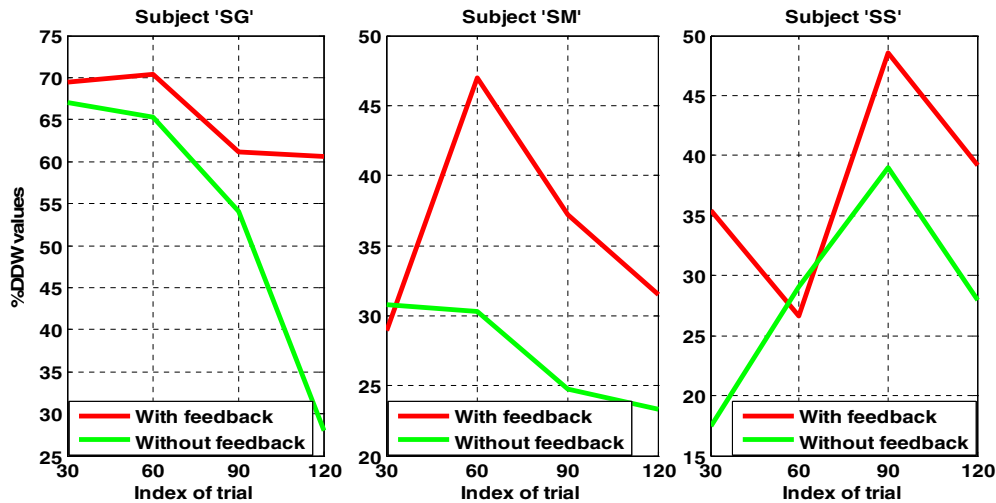
Figure 11. Percentage DDW values for subjects SG, SM and SS with and without feedback.
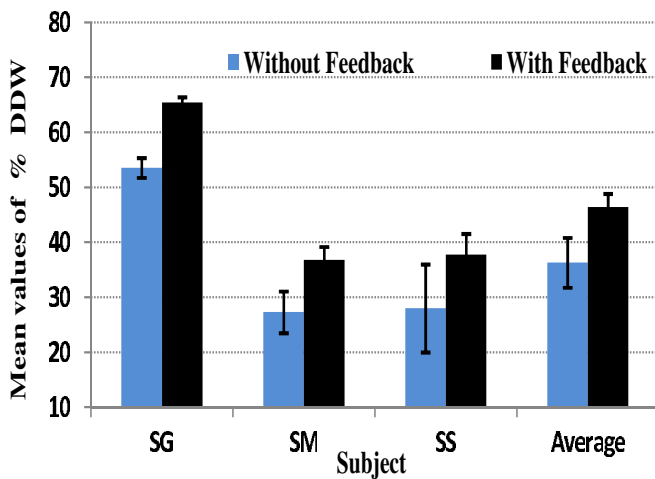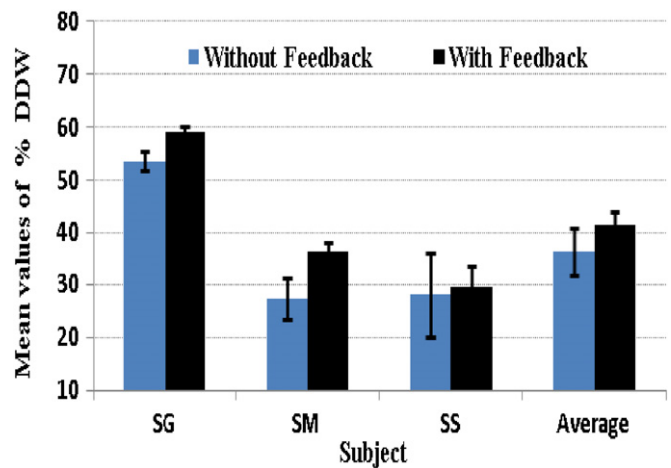

Figure 12. For adaptive evaluation.

Figure 13. For static evaluation.

In order to present the variation in DDW with feedback, the average values of % DDW values for all subjects are computed and plotted. Figures 12 and 13 represent the average % DDW values for EEG recordings with and without feedback for EEGs for the three subjects in session 3, in the adaptive and static recordings, respectively. Comparing the % DDW values with and without feedback given in figures 12 and 13, the percentage increase in average % DDW values over three subjects with feedback is found to be 21.88% and 12.80% in adaptive and static methods, respectively. This study clearly shows that visual feedback in online experiments makes the subject optimize his or her strategy of thinking and results in an increased percentage DDW. As the presence of feedback influences the variation in DFCs, the adaptation of these informative frequency components becomes essential in BCI experiments with feedback.

From the online and offline experimental analysis, it is observed that the classification accuracies can be improved by updating the DFC and bandpass filters adaptively over time. During calibration, three calibration model parameters are developed that comprises the discriminative bands,

CSP projection matrix *W* (or spatial filter) and classifier model. The same classifier hyperplane and CSP matrix are applied throughout the evaluation sessions in SWSSP. The frequency bands and the classifier are updated in AWSSP. The experimental results emphasize the fact that discriminative bands play a significant role in the BCI system even though the weights of channels obtained by the CSP matrix are kept fixed all throughout the analysis. If two discriminative bands cannot be estimated from a certain set of DW values, a possible enhancement of system protocol can be made by selecting the alpha and beta bands which generally appear in the range of 8–13 and 14–18 Hz, respectively [12, 13, 15]. This setting will be helpful in handling real time studies.

Also, for real time applications, the design of filters using the coefficient decimation approach can reconfigure the frequency bands at a reduced computational complexity. However, updating the spatial filter *W* and classifier model will further improve the classification accuracy and new adaptive methods are necessary for better results. A real time robust BCI system should be able to track the time, frequency and spatial domain non-stationarities of the EEG

signal adaptively. In the preliminary online experiments, we have used the supervised updating strategy to estimate the DW values over time and retrain the classifier. In future, we will be focusing on effective unsupervised updating methods for the frequency/spatial filters and classifier model to achieve further performance improvement [28–30].

6. Conclusion

In EEG-based BCI studies, the motor imagery patterns have been successfully used to provide a direct communication pathway from brain to computer. In order to accurately classify the different motor imagery activities in a BCI, it is important to select the subject-specific DFCs. Even though the variability of these DFCs between subjects has been discussed in the literature, their variation over time is hardly discussed. Therefore, we analyze EEG signals recorded on different days and investigate the consistency of DFCs during motor imagery over various sessions. In the study, it is found that the DFCs vary from session to session. Hence, we propose a new adaptive method, AWSSP, that tracks the variability in DFCs adaptively in a BCI framework. It is done by continuously estimating the variations in the discriminative weight values of DFCs and reconfiguring the subject-specific bandpass filters. In offline and online experiments, AWSSP yields significantly better classification accuracies than the BCI scheme that employs the static DFCs. The performance improvement offered by AWSSP over SWSSP emphasizes the importance of addressing the spectral non-stationarities in the EEG signal during motor imagery tasks. The study of the effect of visual feedback on the DW values of frequency components also emphasizes the requirement of updating the discriminative frequency components over time. Further work is needed to optimize the unsupervised adaptation techniques and also to improve the updating strategies in time, frequency and spatial domains.

Acknowledgments

References

[1] Gerven M *et al* 2009 The brain–computer interface cycle *J. Neural Eng.* **6** 041001

[2] Wolpaw J R, Birbaumer N, McFarland D J, Purftscheller G and Vaughan T M 2002 Brain computer interfaces for communication and control *Clin. Neurophysiol.* **113** 767–91

[3] Lotte F, Congedo M, Lecuyer A, Lamarche F and Arnaldi B 2007 A review of classification algorithms for EEG-based brain–computer interfaces *J. Neural Eng.* **4** R1–13

[4] Cheng M, Gao X, Gao S and Dingfeng X 2002 Design and implementation of a brain–computer interface with high transfer rates *IEEE Trans. Biomed. Eng.* **49** 1181–6

[5] Liua G, Huanga G, Menga J and Zhu X 2010 A frequency-weighted method combined with Common Spatial Patterns for electroencephalogram classification in brain–computer interface *Biomed. Signal Process. Control* **5** 174–80

[6] Schalk G 2008 Brain–computer symbiosis *J. Neural Eng.* **5** 1–15

[7] Yang B h, Yan G z, Yan R g and Ting W 2007 Feature extraction for EEG-based brain–computer interfaces by wavelet packet best basis decomposition *J. Neural Eng.* **3** 251–6

[8] McFarland D J and Wolpaw J R 2008 Sensorimotor rhythm-based brain–computer interface (BCI): model order selection for autoregressive spectral analysis *J. Neural Eng.* **5** 155–62

[9] Allison Z, Brunner C, Kaiser V, Muller-Putz G R, Neuper C and Pfurtscheller G 2010 Toward a hybrid brain–computer interface based on imagined movement and visual attention *J. Neural Eng.* **7** 026007

[10] Naeem M, Brunner C, Leeb R, Graimann B and Pfurtscheller G 2006 Separability of four-class motor imagery data using independent components analysis *J. Neural Eng.* **3** 208–16

[11] Wolpaw J R, Birbaumer N, Heetderks W J, McFarland D J, Peckham P H, Schalk G, Donchin E, Quatrano L A, Robinson C J and Vaughan T M 2000 Brain–computer interface technology: a review of the first international meeting *IEEE Trans. Rehabil. Eng.* **8** 164–73

[12] Pregenzer M and Purftscheller G 1999 Frequency component selection for an EEG-based brain to computer interface *IEEE Trans. Rehabil. Eng.* **7** 413–9

[13] Pfurtscheller G and Neuper C 1997 Motor imagery activates primary sensorimotor area in humans *Neurosci. Lett.* **239** 65–8

[14] Guger C, Ramoser H and Pfurtscheller G 2000 Real time EEG analysis with subject specific spatial patterns for a brain–computer interface *IEEE Trans. Rehabil. Eng.* **8** 447–56

[15] Blankertz B, Tomioka R, Lemm S, Kawanabe M and Muller K R 2008 Optimizing spatial filters for robust EEG single trial analysis *IEEE Signal Process. Mag.* **25** 41–56

[16] Ramoser H, Muller-Gerking J and Pfurtscheller G 2000 Optimal spatial filtering of single trial EEG during imagined hand movement *IEEE Trans. Rehabil. Eng.* **8** 441–6

[17] Dornhege G, Krauledat M, Losch F, Curio G and Muller K R 2006 Combined optimization of spatial and temporal filters for improving brain–computer interface *IEEE Trans. Biomed. Eng.* **53** 2274–81

[18] Lemm S, Blankertz B, Curio G and Muller K R 2005 Spatio-spectral filters for improving the classification of single trial EEG *IEEE Trans. Biomed. Eng.* **52** 1541–8

[19] Novi Q, Guan C, Dat T H and Xue P 2007 Sub-band common spatial pattern for brain–computer interface *Proc. 3rd Int. Conf. on Neural Engineering of IEEE Engineering in Medicine Biology Society (EMBS)* pp 204–7

[20] Ang K K, Chin Z Y, Zhang H and Guan C 2008 Filter bank common spatial pattern (FBCSP) in brain–computer interface *Proc. IEEE Int. Joint Conf. on Neural Networks* pp 2390–97

[21] Kavitha P T, Guan C, Lau C T, Vinod A P and Ang K K 2009 A new discriminative common spatial pattern method for motor imagery brain–computer interfaces *IEEE Trans. Biomed. Eng.* **56** 2730–3

[22] Kavitha P T, Guan C, Lau C T and Vinod A P 2008 An adaptive filter bank for motor imagery based brain–computer interface *Proc. 30th Annual Int. Conf. of IEEE Eng. in Medicine and Biology* pp 1104–7

[23] Mahesh R and Vinod A P 2008 Coefficient-decimation
     approach for realizing reconfigurable finite impulse
     response filters *Proc. 2008 IEEE Int. Symp. on Circuits and
     Systems* pp 81–84

[24] Mahesh R and Vinod A P 2011 Low complexity flexible filter
     banks for uniform and non-uniform channelization in
     software radios using coefficient decimation *IET Circuits
     Devices Syst.* at press

[25] Lin M, Vinod A P and See C M S 2009 A new flexible filter
     bank for low complexity spectrum sensing in cognitive
     radios *J. Signal Process. Syst.* **62** 205–15

[26] Cranstoun S D, Ombao H C, Sachs R, Guo W and Litt B 2002
     Time-frequency spectral estimation of multichannel EEG
     using the Auto-SLEX method *IEEE Trans. Biomed. Eng.*
     49 988–96

[27] Leeb R, Lee F, Keinrath C, Scherer R, Bischof H
     and Pfurtscheller G 2007 Brain–computer communication:
     motivation, aim and impact of exploring a virtual apartment
     IEEE Trans. Neural. Syst. Rehabil. Eng. **15** 473–82

[28] Vidaurre C, Schloogl A, Cabeza R, Scherer R
     and Pfurtscheller G 2006 Fully on-line adaptive BCI *IEEE
     Trans. Biomed. Eng.* **53** 1728–31

[29] Bai O, Lin P, Vorbach S, Floeter M K, Hattori N and
     Hallett M 2008 A high performance sensorimotor beta
     rhythm-based brain–computer interface associated with
     human natural motor behavior J *J. Neural Eng.*
     5 24–35

[30] Shenoy P, Krauledat M, Blankertz B, Rao R P and Muller K R
     2006 Towards adaptive classification for BCI *J. Neural Eng.*
     3 13–23